DESIGNING WEAVING PATTERN AND ENGINEERING MULTILAYER STRUCTURE OF NYLON-ACRYLIC FABRIC UTILIZING IN TRIBOELECTRIC NANOGENERATOR

Suchanat Navatragulpisit[1], Praophansupa Krailadsirirattna[1], Rawiwan Khwanming[1], Satana Pongampai[2], Suwan Plaipichit[3], Surawut Wicharn[3], Phakkhananan Pakawanit[4], Naratip Vittayakorn[5] and Thitirat Charoonsuk[1,*]

Received: August 28, 2024; Revised: December 03, 2024; Accepted: December 03, 2024

Abstract

In the contemporary era, the textile triboelectric nanogenerator (T-TENG) has sparked interest to be a powerful energy supply for small electronic devices and electronic component in next generation of electronic textiles. Most T-TENG is developed by adding other materials to fabric or cloths that probably limit the comfortable use. Fabrication of conformable fabrics with high triboelectric outputs remains challenging. This research is firmly focused on the development of fully-fabric T-TENG by employing woven nylon-acrylic fabrics as the main contact material and designing a weaving pattern together with engineering a multi-layered structure to amplify its electrical efficiency. Based on the experimental results, different weaving patterns provided different electrical output values owing to its different contact surface areas. The matt weave pattern can yield the best electrical output regarding the extreme deformations. A further significant enhancement in T-TENG's performance is consistent with inserting polymer intermediate layer. Adding ball-fiber and kapok serves as a synergetic charge-trapping interlayer, rendering a high triboelectricity of both open circuit voltage (V_{OC}) and short circuit current (I_{SC}) for 3 to 8 times higher than that of nylon-acrylic single layer. Finally, the multilayer fabric T-TENG is integrated with the long-sleeved garments and provide output enough to fully-charge the 0.22 µF and 0.33 µF capacitors together with brightening 30 LEDs. Finally, this work demonstrates a potential way with simple procedures in achieving fully-fabric T-TENG for small-scale energy sources that can harvest biomechanical energy to power electronic component for approaching the real application in E-textile systems.

[1] *Department of Materials Science, Faculty of Science, Srinakharinwirot University, Bangkok, Thailand. E-mail: minescn24@gmail.com; praophansupa.kra@g.swu.ac.th; rawiwan.khwanming@g.swu.ac.th; thitiratc@g.swu.ac.th[*]*

[2] *Department of Physics, Faculty of Science, King Mongkut's University of Technology Thonburi, Bangkok, Thailand. E-mail: satana.pong@kmutt.ac.th*

[3] *Department of Physics, Faculty of Science, Srinakharinwirot University, Bangkok, Thailand. E-mail: suwanp@g.swu.ac.th; surawutw@g.swu.ac.th*

[4] *Synchrotron Research and Applications Division, Synchrotron Light Research Institute, Nakhon Ratchasima, Thailand. E-mail: phakkhananan@slri.or.th*

[5] *Advanced Materials Research Unit, School of Science, King Mongkut's Institute of Technology Ladkrabang, Bangkok, Thailand. E-mail: naratip.vi@kmitl.ac.th*

[*] *Corresponding author*

DOI: https://doi.org/10.55766/sujst9981

Keywords: **E-textiles; Insulating polymer; Multilayer structure; Triboelectric nanogenerator; Woven fabric**

Introduction

In today's world, technology and innovation are indispensable for enhancing human life. Leading the clothing and textile which are one of necessities for human also rise to develop by embedding the electronic components inside, as known as electronic textiles (e-textiles) (Younes, 2023). However, traditional E-textiles are bulky and heavy rely on batteries, which need to be used as the primary power source to drive those embedded electronic components. In addition to the inconvenient use, the battery system also comes with clear limitations, including the need for frequent recharging within a short lifetime without environmentally friendly at the end of life. Thus, the search for alternative energy sources has become an intriguing avenue of research. Among several kinds of energy harvesting, *i.e.,* wind, water, and solar power, mechanical energy harvesting (MEH) devices, a field focused on converting environmentally mechanical energy into electricity, has witnessed significant development and remain crucial challenges (Charoonsuk *et al*., 2021a; Ukasi *et al*., 2024). Herein, one of the advanced MEH devices which has high energy conversion efficiency, namely triboelectric nanogenerator (TENG) is getting attention. TENG can transform mechanical energy into electrical energy through the contact and separation of two different materials, inducing charge transfer and generating an electric current (Zhu *et al*., 2015; Charoonsuk *et al*., 2021b). The electric current generated from TENG is sufficient to power small with low power-consumption electronic devices. Over the past decades, various materials, including metals, ceramics, and polymers, can be utilized in TENG devices not even fabric-based materials. The selected fabric materials like nylon (Bairagi *et al*., 2022), cotton (Zhu *et al*., 2019), carbon fiber (Yang *et al*., 2018), polyethylene terephthalate (PET) (Zhao *et al*., 2016), polytetrafluoroethylene: PTFE (Teflon) (Chen *et al*., 2018), and polyacrylonitrile: PAN (Acrylic) (Sun *et al*., 2020), have become interested with specific properties of being lightweight, flexible, and moldable to match the requirements of textile technology. Based on the literature, Yanhua Liu and the team focused on materials selection by choosing materials from triboelectric series to develop E-textiles, and showed the potential of using acrylic to serve as main negative friction layer due to its electron-withdrawing ability relating to a main functional group of nitrile (-C≡N) (Liu *et al*., 2020). Meanwhile, containing amide group ($-NH_2$) in the chemical structure of nylon responses to its high electron-donating ability. Thus, using nylon and acrylic fabric to be material pair is now focused. In 2014, Tao Zhou *et al*., fabricated acrylic based TENG within freestanding mode to provide output efficiency of open circuit voltage (V_{OC}) and short circuit current (I_{SC}) ~100 V and ~1 μA (Zhou *et al*., 2014). Also, a study of Xiao Peng and the team reported the output performance of TENG by using nylon and acrylic coated with gold as main friction materials. The nylon-acrylic TENG demonstrated V_{OC} of approximately 420 V and I_{SC} in range of 1.8 to 9.5 μA (Peng *et al*., 2021). Recently, Paosangthong et.al. used nylon fabric and Teflon fabric to fabricate a T-TENG device, providing the output efficiency of ~200 V and ~0.80 μA (Paosangthong *et al*., 2019). Based on the literature, both nylon and acrylic can be optimum material pair for using as contact materials in T-TENG, but the output current is too low for being small power supply. According to this issue, many researchers have devised ways to improve the output current especially for T-TENG devices. By considering the simple structure of TENG, there are two main component layers, composing of charge-generating layer for creating the charges and charge-collecting layer for transporting the created charges through the load. Improving charge-generating has been first focused. In a previous study by J. Jeong et.al. (Jeong *et al*., 2019), having different weaving patterns of cotton fabric between plain weave and 2/1 twill weave revealed the different V_{OC} of approximately 1.59 V and 12.47 V. Next, Somkuwar *et al*. (2020), also tried to compare between plain weave and 5/1 twill weave for T-TENG and found the similar trend of results. The different V_{OC} and I_{SC} of 2.52 V and 3.68 μA for plain weave fabric and 10.93 V and 7.04 μA for the 5/1 twill weave could be generated, confirming the significantly impact of weaving pattern on the output efficiency of T-TENG. Based on the literature, even though simple weaving pattern making can suggest a potential trend in developing of T-TENG from fabric-based materials, the experiment with nylon and acrylic has not been done and more pattern with scientific discussion still needs to be full-filled in this case. Moreover, the challenges still exist in terms of undesirable output current due to the charge's loss by recombination between friction surface and electrode. Therefore, another way to enhance the electrical output has been studied. One effective method to eliminate the limitation of recombination is doing in structural design by designing TENG into multilayer-structure. Studies of adding charge-trapping layer by inserting the insulating interlayer are relatively new (Xie *et al*., 2021). Previous studies have done on the polymer TENG and reported that inserting polymer film that contain the aromatic rings in main chains, *i.e.*, polyimide (PI) (Feng *et al*., 2017), and polystyrene (PS) (Cui *et al*., 2016), between the PVDF layer and charge-collecting layer can enhance the electrical output signal by 7 to 9 times higher than that of the device without inserting interlayer. Adding a PDMS film for interlayer also successfully increased the output power of PVDF TENG by 178 times without any destroying high stretchability of the stretchable TENG (Kim *et al*., 2018). Even though the multilayer structural design by inserting charge-trapping interlayer has been done on polymer films, it has not been done in field of textiles. Therefore, studies from previous research becomes motivation in this work to pay attention in addition to modify the charge-generating layers in T-TENG. The fabrication of textile multilayer structure with integrating the charge-trapping layer by using simple process are undertake challenging.

This research aims to develop the nylon-acrylic T-TENG by using combination methods consisting of fabricating suitable weaving pattern and multilayer structural design. The various weaving patterns are explored to assess their impact on the total surface contact area relative to the electrical output characteristics of T-TENG. Furthermore, another aims to enhance the electrical performance by engineering a multilayer structure with integrating the charge-trapping layer using four different kinds of fibers, including ball-fiber, synthetic fiber, microgel and kapok. The optimum condition could be achieved by providing the electrical output enough to further test and use for practical application. The scientific discussion about output efficiency relative to material characterization and operation mechanism for single layer and multilayer T-TENG is provided regarding sliding operation mode. Also, this fully-fabric T-TENG technology is successfully applied in the circuit board to investigate potential output for applications such as chargeability and ability for driving small electronic devices.

Experimental Procedures

Weaving Fabrics Process

In this work, by following the results from calculations, the fabrics were weave by using nylon/stainless steel thread and acrylic/stainless steel thread within 3×3 cm^2 size. The nylon and acrylic thread act as weft yarn, while a warp yarn and electrode are using stainless steel thread. The fabrics were weave in 3 different weaving pattern including plain weave, 2/2 twill weave and matt weave irregular by using 6×7 cm^2 size of small loom.

Fabrication of Multilayered Woven Fabric

A multilayered woven fabric was prepared using nylon and acrylic fabric, sewn into a size of 3×3 cm with a gap in the middle. Subsequently, all the previously prepared fibers, including ball fiber, synthetic fiber, microgel fiber, and kapok fiber, were inserted into the middle between two layers of frication layers to obtained multilayer-nylon fabric and multilayer-acrylic fabric.

Fabrication of Triboelectric Nanogenerator (TENG) Device

In this work, the TENG apparatus encompasses within the linear sliding mode. The TENG device consists of two contact layers composing of 3×3 cm^2 fabric with three different weaving patterns of nylon/stainless steel for the tribo-positive friction layer and acrylic/stainless steel for the tribo-negative friction layer. Both sides of friction layer are attached with glue fabric/CNT composite as electrode. Then, the two electrodes are connected to an electrical wire.

Characterization and Electrical Output Measurement

Attenuated Total Reflection-Infrared Spectroscopy (ATR-IR, Shimadzu IRTracer-100) was employed to observe their functional groups and chemical bonding of the nylon, acrylic fabric, and all fiber. To assess the overall internal structure of all fiber and estimate fiber diameter, synchrotron radiation X-ray tomographic microscopy (SR-XTM) was conducted at SLRI Thailand. After getting contrast images frame from SR-XTM, the high-resolution three-dimensional (3D) images of all fiber were visualized using the Drishti software. For evaluating the electrical output performance of the woven fabric-based TENG, the output signal waveforms including open-circuit voltage (V_{OC}), short-circuit current (I_{SC}), and maximum output power (P_{max}) were conducted by using an oscilloscope (DSO-X

2012A, Keysight) and the digital multimeter (DM3058E model, Rigol).

Result and Discussion

Single Layer T-TENG Fabrication

Surface Contact Area Calculation of Woven Fabric With Different Weaving Pattern

At the beginning, data of the diameters for nylon, acrylic, and stainless-steel yarns was collected to calculate the surface area of fabric samples. The size of fabric samples was set at 3×3 cm^2 and the representative dimension parameters are shown in Figure 1(a). The formula for calculating the total contact surface area based on the research conducted by Kavita and Abdel-Fattah (2011) can be found in supplementary information in accordance with equation (S1)-(S3) (Kavita and Abdel-Fattah, 2011), where p_1 and p_2 is a warp and weft spacing (1/number of warp or weft yarns). The d_1 and d_2 represent the diameter of warp and weft yarns while C_1, C_2 and C_f refer to the surface contact area of warp yarns, weft yarns and total surface contact area, respectively. The total surface contact area from the research of Nazmul Hossain method (Saleem *et al*., 2021) was also studied for secondary confirming the calculated results of contact area. The Nazmul's equation can also be found in supplementary information of equation (S4)-(S6). Based on the surface area calculations derived from the research of Kavita and Abdel-Fattah, as well as Nazmul Hossain method that were adopted for the total surface contact area competition of woven fabric with different weaving patterns. Those 9 different weaving patterns of fabric, according to the mock drawing in Figure 1(b), were interesting because of their commercially famous in the fabric market. It was found that the results of calculated contact surface area of different patterns from both methods appeared in the same trend, are tabulated in Table 1.

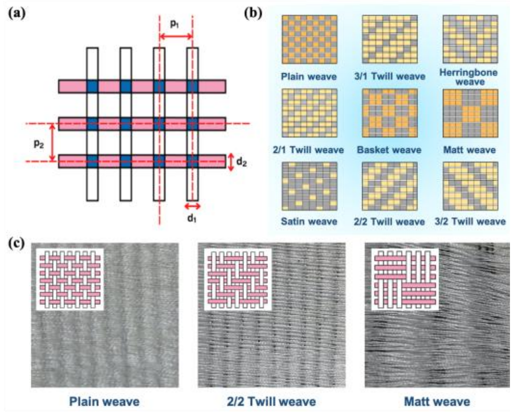

Figure 1. (a) Illustration of surface contact area and calculation of contact surface area with variables specified (b) Overall weaving patterns (c) Digital photograph and diagram of Plain weave, 2/2 Twill weave, Matt weave

The calculated results illustrated that different weaving pattern of fabric is directly relative to the different total surface contact area, arranging in the examples from containing low-to-high surface area by following the plain weave, 2/2 twill weave and matt weave that the surface contact area of 0.13%, 0.25% and 0.39% was found respectively. The total surface contact area of these three different patterns were confirmed again by Nazmul Hossain method of calculation, which exhibited a consistent trend in their total contact surface area with previous calculation method. The Nazmul's calculation results are also listed in Table 1 that the plain weave, 2/2 twill weave, and matt weave have total surface contact area values of 5.86, 6.29, and 6.37 yarn/inch^2, respectively. Therefore, the result of calculation can confirm the effect of different weaving patterns to total surface contact area, providing possibility to affect also with electrical output performance. To further study the effect of

Table 1. Ratios of total contact surface area for different weave patterns from the research of Kavita Mathur and their team

Weaving pattern	Total surface contact area Kavita and Abdel-Fattah (2011) (%)	Total surface contact area Nazmul Hossain et.al. (yarns/inch^2)
Plain weave	0.13	5.86
2/1 twill weave	0.20	6.06
Herringbone weave	0.22	6.11
2/2 twill weave	0.25	6.29
3/1 twill weave	0.26	6.30
Basket weave	0.28	6.32
3/2 twill weave	0.30	6.34
Satin weave	0.31	6.35
Matt weave	0.39	6.37

different weaving patterns on electrical output of T-TENG, the three patterns that contain lowest, medium, and highest surface contact area have been selected in this experiment, that was the plain weave, 2/2 twill weave and matt weave pattern, respectively. Then, the nylon and acrylic yarn were weaved within the three different patterns together with stainless steel yarn for use as an electrode (Figure 1(c)). The woven fabric samples were fixed equally within a 3×3 cm^2 of dimension for fabricating the T-TENG.

Electrical Output Measurement of Woven Fabric With Different Weaving Pattern

Before measuring and comparing the output efficiency of each pattern, the two theories is brough to be understood for selecting materials pair: (1) inductive effect (Kingsbury, 2019) and (2) the triboelectric series (Liu *et al*., 2020). The inductive effect refers to the phenomenon wherein a permanent dipole in molecule arises due to the unequal sharing of the bonding electrons that is usually used to explain the electron-donating and accepting ability of functional groups in organic materials and polymers. Meanwhile, the triboelectric series is well known for considering the material selection in fields of TENG that basically uses the Intermolecular Electron Cloud Overlap Transfer (IECOT) model (Lin *et al*., 2020) to explain the distinct electron-donating and -receiving properties of materials. In this work, the main material fabrics are acrylic and nylon with the scientific name of polyacrylonitrile and polyamide. The C ≡ N acts as a main functional group of polyacrylonitrile that is categorized as electron withdrawing group (-I effect) by containing ability to draw electron density towards itself. Meanwhile, the polyamide contains N-H and C=O-R as functional groups. N-H is clearly positioned at +I affect that can releasing electron easily.

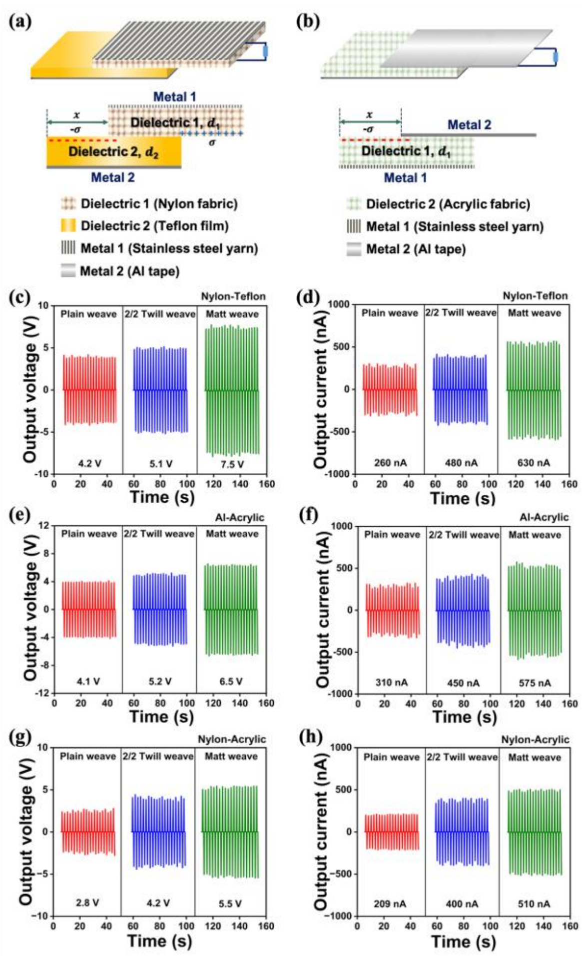

Figure 2. Structural T-TENG models for (a) dielectric-to-dielectric and (b) metal-to-dielectric sliding mode, (c)-(d) V_{OC} and I_{SC} of nylon fabric-Teflon, (e)-(f) Al-acrylic fabric, and (g)-(h) nylon-acrylic fabric with plain weave, 2/2 twill weave and matt weave

Even though the C=O-R is positioned in the -I side, however, it still has low ability to withdraw electron as compared to C ≡ N of polyacrylonitrile. Also, the triboelectric series that contains the ranking of electron donating and accepting ability of the most polymers (Liu *et al*., 2020), clearly shows the position of acrylic (polyacrylonitrile) in the negative side (electron acceptor) and nylon (polyamide) in the positive side (electron donor). The distance between them in the chart is quite far, thus confirming the possibility to use acrylic as negative and nylon as positive friction layer for T-TENG in this work. Therefore, to find the optimum condition in the first part of electrical output measurement, nylon and acrylic with three different weaving patterns of each was tested within the two materials pair of nylon-Teflon and acrylic-Al systems. Since nylon contains electron donating ability existing in positive side of triboelectric series, the Teflon films is therefore selected to be its negative side. According to the previous work, Teflon was basically used as standard negative layer to pair with the sample of positive layer for testing the TENG's output efficiency owing to its highest ability to gain electron listed in triboelectric series (Kim *et al*., 2017). The simple structure in the drawing diagram is illustrated in Figure 2(a). Meanwhile, the acrylic exists in the negative side of triboelectric series, Al thin film was chosen to be tribo-positive side for matching with acrylic woven fabric T-TENG, as shown by simple structure in Figure 2(b). Regarding the triboelectric operation, the lateral sliding (LS) mode T-TENG is taken in terms of the dielectric-to-dielectric and metal-to-dielectric TENG model's category, according to Figures 2(a-b). The model for the kind of dielectric-to-dielectric was used for finding optimum condition of woven nylon T-TENG. The top section is composed of nylon woven fabric which acts as tribo-positive layer sewing with stainless steel yarn as electrode. The Teflon film serves as a tribo-negative layer contacting with Al tape electrode, existing in the bottom section of the device. In the experiment, Teflon and Nylon were used as a triboelectric pair at the same sample size of 3×3 cm^2 and d = 500 μm. The basic structure in Figure 2(a) is displayed including dielectric 1 (D1; woven nylon fabric), and dielectric 2 (D2; Teflon). Both D1 and D2 are attached to metal electrode, M1 and M2, located at the top and bottom, respectively. As shown representatively in drawing diagram, the width of the whole materials is much larger than the thickness, which represented by d_1 and d_2. The uniformly distributed charge on the inner surfaces is reasonably assumed. During separation between D1 and D2, the different types of surface charge induce at the non-overlapped regions due to the triboelectrification (Niu *et al*., 2013; Niu and Wang, 2015). For the operation, the top-part of T-TENG slides through the longitudinal direction while the bottom part is fixed. The lateral separation distance is defined as x, and the surface charge density on D1 and D2 are denoted as +σ and –σ. The width (w = 3 cm) of the whole dielectric layer (3 cm) is much larger than its thickness (d_1 = 0.1 mm or 100 μm and d_2 = 0.5 mm or 500 μm). It is assumed that the triboelectric charges are uniformly distributed across the material surfaces. After connection of M1 and M2 with conductive wires, the charges would be transferred. The number of transferred charges denotes as Q_{SC} the total charge amount on M1 and M2 is represented by $-Q_{SC}$ and Q_{SC}. The L-S mode T-TENG within metal-to-dielectric category (Figure 2(b)) is different by disappearing of the D1 layer. The M1 acts not only as the top electrode but also acts as the triboelectric layer itself to donate the electron to the D2 layer. During the separation, the uniform tribonegative charges, defining as –σ, can be produced at non-overlapped regions and the different sign with same amount would be created on the M1 (Niu and Wang, 2015). For both cases, the triboelectric charge on the overlapped region is canceled because of charge neutrality during the contacting process. The total amount of σ is expressed by σwx (Niu *et al*., 2013; Niu and Wang, 2015). To deliver the output performance of the TENG, the potential difference (V) contains the specific relationship with Q_{SC} and x. The V-Q-x relationship can be expressed as illustrated in supplementary information.

According to the theoretical understanding for the V-Q-x relationship, the output performance of the T-TENG in this work is firstly determined basically in terms of V_{OC} and I_{SC}. The electrical output signal waveforms of woven fabric T-TENG consisting with nylon woven fabric in various weaving patterns paired with commercial Teflon are shown in Figures 2(c-d). By comparing the output efficiency of nylon woven fabrics within different weaving patterns of plain weave, 2/2 twill weave, and matt weave, the normal plain weave pattern provides the V_{OC} and I_{SC} of 4.2 V and 260 nA. Meanwhile, the highest Voc and I_{SC} was generated by matt weave pattern of 7.5 V and 630 nA, which is 1.7 times and 2.4 times higher than the plain weave pattern. It can be seen clearly that the electrical output shows consistency with the results of contact surface area calculation. The higher total surface contact area can significantly enhance the output efficiency of woven fabric-based T-TENG. It can be concluded that for the positive side using nylon, the matt weave pattern shows the highest surface contact area, as tabulated in

Table 1, compared with other pattern, increasing proportionally with the output efficiency that led to the highest values in this work. The different pattern was also studied within the acrylic side by pairing with the Al thin-film tape as mentioned above in metal-to-dielectric system. The electrical output was also studied according to Figures 2(e-f). The results show that the V_{OC} and I_{SC} of plain weave pattern reached about 4.1 V and 310 µA. For 2/2 twill weave pattern, the Voc and I_{SC} were gradually increase to 5.2 V and 450 µA. Meanwhile matt weave pattern reaches the highest Voc and I_{SC} of 6.5 V and 575 µA which is higher than the output efficiency of plain weave 1.5 times and 1.3 times. Furthermore, for the full-fabric system T-TENG, the woven nylon and acrylic fabric in different patterns was paired to fabricate the T-TENG. As illustrated in Figure 2(g-h), the similar trend of V_{OC} and I_{SC} could be observed to matt >2/2 twill > plain weave by generating 5.5 V>4.2 V>2.8 V, and 510 nA>400 nA >209 nA, respectively. The results can prove that the waving pattern has a direct effect on the electrical output efficiency for any fabric T-TENG influencing by the surface contact area. The weaving pattern that can provide the highest surface area also provides the highest electrical output efficiency for T-TENG.

Figures 3(a-b) illustrate the structure and the mechanism of T-TENG operation employing the sliding working mode that converts mechanical energy into electrical energy by interaction of two woven fabrics involving in combination process of triboelectrification and electrostatic induction. According to the T-TENG structure (Figure 3(a)), the top section is composed of nylon/stainless steel woven fabric that nylon acts as tribo-positive layer while stainless steel yarns are utilized as electrode. The acrylic/stainless steel fabric serves as a tribo-negative layer is pasted in the bottom section. Nylon/stainless steel and acrylic/stainless steel fabric were woven in different patterns using fabric as weft and stainless steel as a warp yarn to study the effect of weaving pattern to its electrical output. In experimental setup, acrylic side was fixed positioned at the bottom while the top position was set to a free moving in longitudinal direction. In the beginning (Figure 3(a)), the nylon and acrylic side are fully contacted with each other *via* complete overlapping. Thus, there is no charge transfer between its electrodes through the load. The only interaction occurred within triboelectrification by exchanging the electrons between nylon and acrylic fabric side. The nylon fabric creates positive tribo-charges, while negative tribo-charges are generated

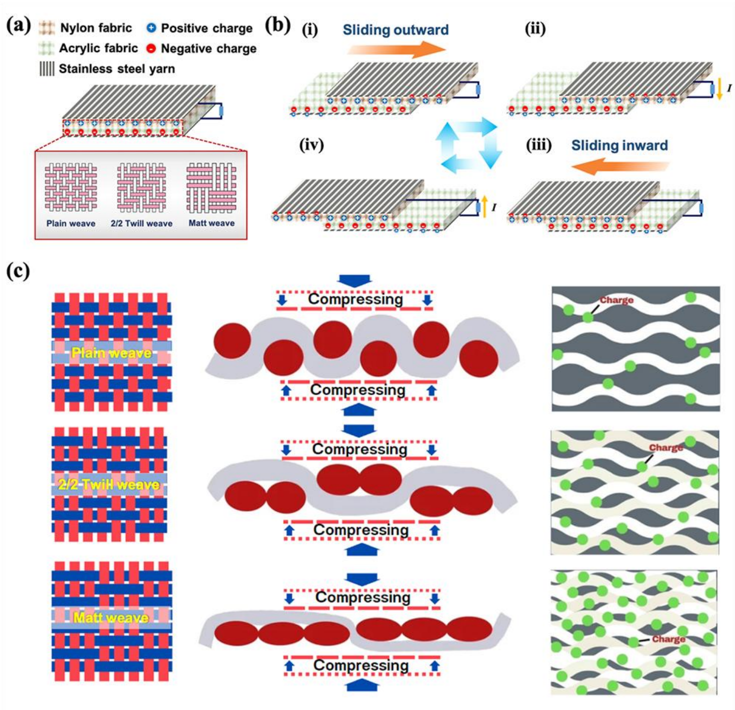

Figure 3. **(a) Schematic diagram of T-TENG structure and (b) operation mechanism in lateral sliding mode, while (c) illustrates the influence of surface contact area on the surface charge generation after receiving the compressive force during T-TENG operation**

on the surface of acrylic fabric. However, the exchange charges are still in electrostatic equilibrium since the positive and negative charges are still equally attract on their surfaces. The state of T-TENG movement is illustrated in Figure 3(b), starting with the outward sliding motion in the *x*-axis direction by applying mechanical force in state (i) - (ii) to occur the electrostatic induction. In Figure 3(b) (i), nylon side on the top slides outward along the weft yarn. Electrostatic induction happens at this state. The charges can flow through the load bringing from weft yarn to the warp electrodes until reaching equilibrium. The charge transfer stops. According to the state (iii) and (iv), the upper substrate slides back to the original position. The charges can be flowed back from the warp electrode at the top to the bottom electrode. The current flowing keeps going until the potential gradient terminates after the contacting of both nylon and acrylic comes to contact fully again. The sliding of T-TENG would be continued in cycles resulting in an alternating current (AC) signal waveform. The influence of contact surface area is illustrated more clearly in Figure 3(c). A higher surface area can generate higher electrical output in terms of both V_{OC} and I_{SC} because a larger surface contact area can generate more charges. According to the operation mechanism, the electrical output of the TENG can be generated only when there is the contact and separation occurrence between two materials surfaces. Therefore, the area that is contacted is one of crucial role. As displayed in Figure 3(c), it is evident that plain weave pattern, which has the smallest surface contact area between each yarn, resulting in a dense fabric structure. When compressive force from the contact sliding motion is applied during testing, the fabric hardly deforms and leading to the minimal contact between the yarns and between the yarn and material pair. So, the charges were lower generated with the lower output signal in both V_{OC} and I_{SC}. Also, the mechanism of surface contact area by compressing the force to 2/2 twill weave pattern was demonstrated. The illustration shows that, when the force is applied, the surface between each yarn can contact each other and generate more charges. In the case of matt weave, which has a larger contact surface area between each yarn that provide less dense compared to plain weave and 2/2 twill weave. Therefore, when the matt weave fabric T-TENG subjects to compressive force, the fabric deforms more than other pattern, increasing the contact between the yarns, generating more charge with the highest output efficiency.

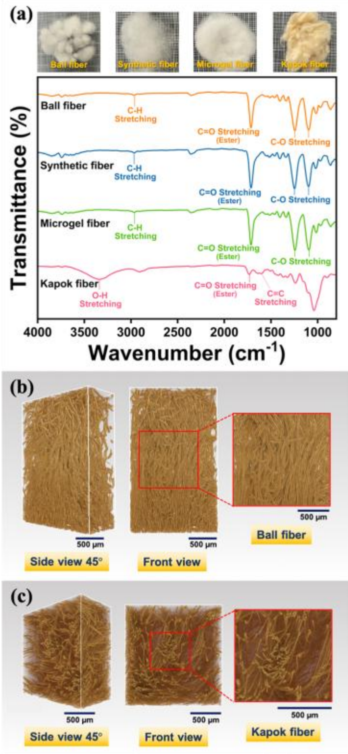

Figure 4. **(a) The IR spectra of the following fiber types: ball fiber, synthetic fiber, microgel fiber, and kapok fiber (b) SR-XTM images of the internal structure for the ball fiber and (c) kapok fiber**

Multilayer T-TENG fabrication

Characteristics and Analysis Specific Four Types of Intermediate Layer Fibers

After the effect of weaving pattern on the electrical output signal was studied, the matt weave pattern for both nylon and acrylic fabric was used for continuing the structural design by adding different types of fiber to be intermediate trapping-layer. Before fabricating the multilayer T-TENG, the functional groups of four types of intermediate layer fibers, comprising of ball fiber, synthetic fiber, microgel fiber, and kapok fiber, were examined by ATR-TR technique to identify the type of polymer molecule. The results are illustrated in Figure 4(a), the ball fiber exhibited characteristic absorption peaks at approximately 2,960 cm^{-1}, corresponding to the stretching vibrations of C-H bonds (C-H stretching). It also displayed absorption peaks at around 1,714 cm^{-1}, aligning with the stretching vibrations of C=O bonds (C=O stretching), indicating the presence of ester groups (Ester group). Additionally, an absorption peak around

1,247 cm^{-1} and 1,097 cm^{-1}correlated with the stretching vibrations of C-O bonds (C-O stretching), also confirming the ester groups. All these results were found to be consistent among ball fiber, synthetic fiber, and microgel fiber. This indicates that all three of these fibers are synthesized from the same polymer, namely, polyester. Notably, these observations are consistent with the findings from previous research conducted by Bhattacharya and their research team in 2014 (Bhattacharya and Chaudhari, 2014) and 2019 (Koto and Soegijono, 2019). However, the kapok fiber shows the IR pattern in a different way. The result of kapok fiber revealed the IR peaks at 3,342 cm^{-1}, corresponding to the stretching vibration of O-H bonds (O-H stretching). Another absorption peak at around 1,728 cm^{-1} matched well with the stretching vibration of C=O bonds (C=O stretching), which is a functional group found in the monosaccharides of hemicellulose within kapok. The peak at approximately 1,594 cm^{-1} belongs to the stretching vibration of C=C bonds (C=C stretching), indicating the presence of aromatic compounds of lignin within kapok (Kartina and Suhaila, 2012). Therefore, it can be concluded that the intermediate layer fibers utilized in this study and research actually comprise fibers from polyester and natural lignocellulosic fibers like kapok.

Comprehensive analysis of fibers was also utilized in this work with the Synchrotron Radiation X-ray Tomographic Microscopy (SR-XTM) technique, renowned for its high-resolution 3D imaging capabilities. The SR-XTM images can reveal the fine nuances of fiber morphology, including diameter, shape, and distribution. Such detailed characterization is instrumental in comprehending the unique properties of these fibers and their potential applications. Herein, the ball fiber is formed from polyester fiber similar to other polyester fiber, *i.e.*, synthetic and microgel fiber that also used in this work. However, according to the result of electrical output measurement in the next section, inserting ball fiber for nylon-acrylic T-TENG can reach the highest performance of electrical output generation. The internal structure compared between ball fiber and kapok fiber is therefore investigated representatively. The SR-XTM technique employs X-rays from a synchrotron light source for scanning and visualizing the three-dimensional internal structure of fibers. As depicted in Figures 4(b-c), the result delves into the intricate details of these fibers, providing valuable insights into their structural attributes. The results in Figure 4(b) emphasized the distinctive characteristic morphology of ball fiber, particularly its thick and large-size fiber structure. Moreover, the analysis revealed bundling within ball fibers, signifying a higher fiber density compared to other fiber types. The average size of ball fibers was calculated using the Fiji - ImageJ software and it was found to be 40.1 ± 8.8 µm. Meanwhile, the SR-XTM image in Figure 4(c) demonstrated that the internal structural of kapok indicated the non-uniform size distributed fiber inside. The average sizes of both large and small synthetic fibers were also measured using the Fiji - ImageJ program. The average size of the kapok fibers was approximately 24.4±14.1 µm. In addition to the molecular types of commercial fibers, the morphological structure may also affect the electrical output which is discussed later in the part of electrical output measurement.

Electrical Output Measurement of Woven Fabric with a Multi-Layered Structural Design

In this work, the efficiency T-TENG is further improved aiming to utilize as close to the real application as possible. The structural design into multilayer structure T-TENG is then focused by inserting intermediate layers between fabric and electrode with commercial fibers that simply find on the textile market, including ball fiber (BF), synthetic fiber (SF), microgel fiber (MF), and kapok fiber (KF) as intermediate layers for a multi-layered structure. The fabric electrode also modified by using the glue-fabric/CNT composite that the optimum condition of CNT can be found on our previous research in 2023 (Khwanming *et al.*, 2023). According to the first part of single layer T-TENG output measurement, the PTFE and Al were used to friction with nylon and acrylic, respectively, because the PTFE is the most negative position in triboelectric series. Even though the Al is posed below nylon in triboelectric series, metals typically tend to donate electrons and Al tape is easy to fabricate as a friction layer in TENG. Also, to further study the performance of multilayer structure compared to single layer T-TENG, the same material friction of PTFE and Al was also used for pairing with multilayer nylon and acrylic system. The study examined the V_{OC} and I_{SC} of multilayer T-TENG with different intermediate fibers. A structure and operational mechanism of multilayer T-TENG was also utilized within the L-S mode. The first T-TENG belonging to nylon-Teflon pair was tested. The primary contact material consists of a multilayer nylon woven fabric, serving as the tribo-positive layer, and Teflon as negative friction layer. Based on the obtained results of V_{OC} and I_{SC} in Figures 5(a-b), a comparison between non-fiber inside or nylon-single layer (N-SL) and nylon multilayer with BF (N-BF), SF (N-SF), MF (N-MF) and KF (N-KF) has been clearly shown. It was obtained that the N-BF T-TENG can achieve the highest of both V_{OC} and I_{SC} about 24.5 V and 4.8 µA that was 3.2 and 7.6 times higher than that of single layer woven fabric. In the case of multilayer acrylic, inserting intermediate layer with BF, SF, MF and KF similar to nylon T-TENG is studied by paring with Al tape. The V_{OC} and I_{SC} by comparison between acrylic-single layer (A-SL) and multilayer of A-BF, A-SF, A-MF and A-KF is presented in Figures 5(c-d). Similarly, the electrical output signal of multilayer acrylic T-TENG could be higher than that of A-SL, demonstrating the effect of intermediate layer. However, the types of intermediate layer showing highest performance are different from the nylon system. In the case of acrylic fabric side, inserting with kapok fiber reached maximum output of the V_{OC} of 21.8 V and I_{SC} of 4.2 µA.

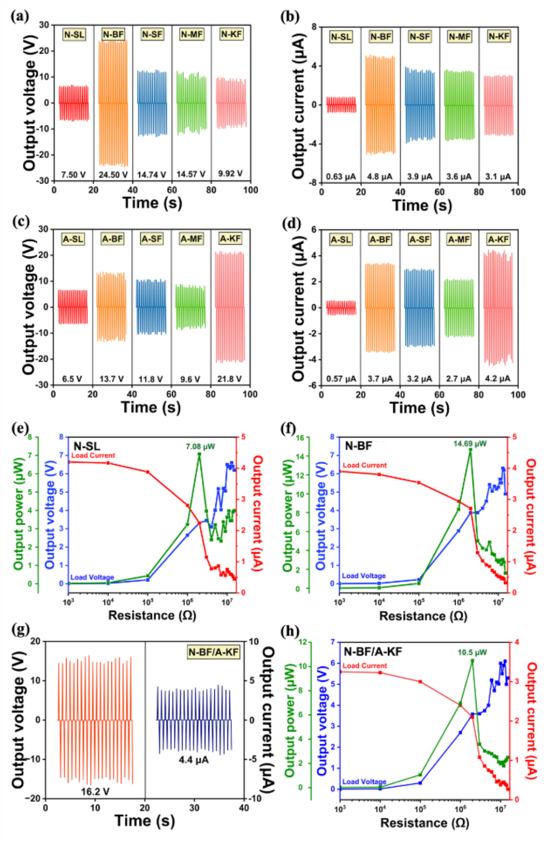

Figure 5. **(a) V_{OC} and (b) I_{SC} of nylon fabric single layer T-TENG compared to the multilayer T-TENG by inserting different of intermediate layers, (c) V_{OC} and I_{SC} of acrylic woven fabric with and without inserting different types of intermediate fiber, (e) P_{max} of multilayer N-BF/Teflon and (f) Al/A-KF T-TENG, (g) V_{OC} and I_{SC}, and (h) the P_{max} of N-BF/A-KF T-TENG**

In triboelectric nanogenerator devices, the introduction of an intermediate layer, also known as a charge-trapping layer, plays a crucial role in capturing charges and preventing the loss of charges. This results in increased charge accumulation within the device, leading to enhanced electrical output and current flow, according to previous research by Menge *et al*. (2020), in 2020. However, the specific materials need to be considered. To test for use in practical applications, matching resistance needs to be checked for finding optimum P or P_{max}. Therefore, the P_{max} of multilayer T-TENG within nylon-Teflon and Al-acrylic systems was examined by connecting the T-TENG device to the electrical circuit by changing the resistance load one-by-one from 100Ω to 15 MΩ and measure the direct voltage, V_{DC} with oscilloscope. The I_{DC} was calculated using equation of I = V/R, simultaneously with calculating P by P = V × I expression. The examined results of V_{DC}, I_{DC} and P for multilayer T-TENG, including woven N-BF/Teflon and Al/A-KF, as a function of load resistance is presented in Figures 5(e-f). Upon increasing the resistance in 100Ω -15 MΩ peried, the V_{DC} increased gradually, meanwhile, the I_{DC} decreased by exactly following the Ohm's law. The P_{max} value can be seen at specific resistance, which is the matching resistance of this T-TENG device. According to the plot between V_{DC}, I_{DC} and R, The P_{max} normally obtained at the point intercept between V_{DC} and I_{DC}. The results can be evident that, the nylon-Teflon system with inserting intermediate layer of BF (N-BF/Teflon), the P_{max} of 7.1 µW is exhibited at specific 2MΩ resistance (Figure 5(e)). In contrast, the multilayer-structure T-TENG with Al/A-KF fabric friction layer achieved the P_{max} of about 14.7 µW at the same resistance value of 2MΩ, as illustrated in Figure 5(f). Moreover, the N-BF and A-KF was brough to fabricate positive and negative layers in T-TENG and investigate the electrical output performance, aiming for utilizing in textile application. The N-BF/A-KF T-TENG demonstrate the AC signal waveforms of V_{OC} = 16.2 V and I_{SC} = 4.4 µA, according to Figure 5(g). The lower output in both V_{OC} and I_{SC} as compared to the N-BF/Teflon and Al/A-KF T-TENG systems is obtained because of the different electronegativity or electron-donating-accepting ability of materials. Nylon has low electron-donating ability when compared to the metal Al, meanwhile, acrylic has low electronegativity (low electron-accepting ability) by comparing with Teflon. Therefore, pairing nylon with Teflon can show higher efficiency and paring acrylic with Al also showed higher efficiency, when both compared to the pairing between nylon and acrylic fabric. However, the full system of fabric TENG still needs to be developed for aiming to the real application. The P_{max} output of N-BF/A-KF T-TENG is shown in Figure 5(h) that the 10.5 μW could be reached at also 2MΩ. The result can demonstrate that even though the full fabric system provides lower efficiency than that of using other materials. The obtained output is not lower than much, it still can be used in terms of T-TENG. Altering the structure with multiple layer fabrication using fiber insertion significantly enhances the output power, providing a promising avenue for device development. This underscores the importance of charge-trapping layers as an effective approach to enhancing and developing electrical output efficiency.

Figure 6(a) illustrates the diagram of multilayer T-TENG structure for applications that composes of multilayer nylon/kapok (N-KF) pairs with multilayer acrylic/ball-fiber (A-BF). Both of them were ironed with fabric/CNT to be their electrode. Basically, charge trapping's ability in polymer insulators for blocking the charge combination can be formed by imperfections in chemical and physical defects, for instance; crosslinking points, amorphous free volume, dangling bonds and functional groups that mostly occurs in the polymer chains (Bairagi *et al*., 2022). The aromatic polymers have the trapping sites in their chemical structures, regarding to the non-uniform of energy levels along their molecular chain. Therefore, in this work, inserting polyester and kapok fibers can be used for blocking the recombination of the charge along their molecules. Polyester contained the aromatic directly in a chain while kapok have the aromatic ring in their lignin component molecules. Figure 6(b) illustrates a schematic diagram of the electron transfer in multilayer T-TENG by representing one side of nylon with ball fiber (N-BF), which is composed of three layers of nylon itself, BF charge-trapping layer and bottom electrode (GF/CNT). After the separation process occurs, the free charges first appear at the interface by making the gradient of the charge concentration. Having intermediated layer by BF can block the charge recombination allowing comfortable electrostatic induction. The small electric field can form between the nylon and bottom electrode, resulting in electron transfer. For single layer TENG, the shallow trapping process by nylon itself probably results in charges disappearance by the combination process near the bottom electrode. In other words, the positive charges are not accumulated on the nylon surface but drift and flow back to combine with negative

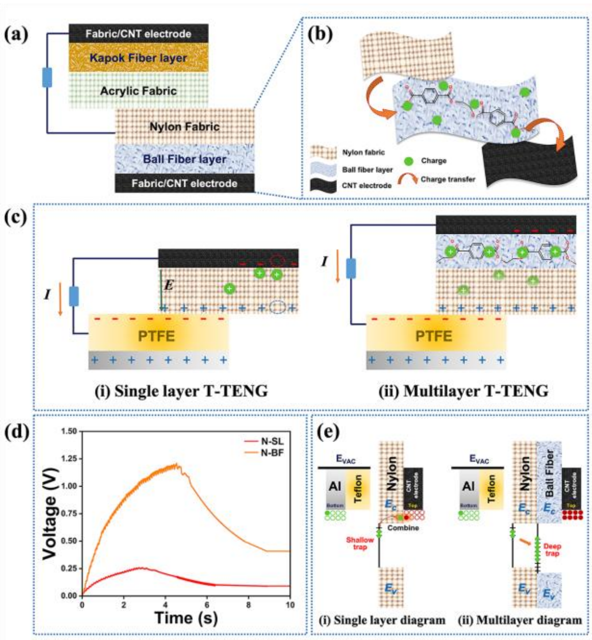

Figure 6. **(a) Schematic illustrations of the multilayer structure T-TENG for application with (b) representative diagram for one side of positive friction layer of nylon with intermediate layer of ball-fiber, (c) the working principle of the charge-trapping layer for blocking the charge-recombination between friction surface and electrode, (d) The surface potential measurement and (d) energy band of single layer compared to multilayer T-TENG**

charges at the electrode, providing a potential decay with incomplete electrostatic induction, as depicted in Figure 6(c) (i). In contrast, inserting NF intermediate layer acts as the charge-trapping sites to trap and block the generated charges from drifting, together with being the deep traps sites to slow down the charge escaping. The creation of the triboelectric charge trapping depth layer provides more opportunity to accumulate the surface charge completely, enhancing the potential difference between electrodes. The schematic diagram of trapping process is illustrated in Figure 6(c) (ii). According to Figure 6(c), the comparison of the charged-discharged curve of voltage was measured representatively comparing between single layer (N-SL) showing in red line and multilayer N-BF T-TENG (orange line). The potentials were measured by constantly sliding motion at 10 Hz. The results demonstrated that the N-SL provides maximum 0.24 V and gradually decreases until releasing almost potential within 3 sec. The N-BF multilayer preserve better potential by holding at 0.39V after 9 sec. The multilayer T-TENG can capture more charges, reaching 5 times higher than that of the single layer T-TENG. The mechanism of charge trapping layer in terms of energy band theory is presented in Figure 6(e). According to Figure 6(e) (i), the positive charges in green dots were generated at the shallow surface of Nylon. The positive charges were temporary stored by combing with the electrons (red dots) at the CNT electrode and formed a weak electric field (Kim *et al*., 2018). In comparison to multilayer, by inserting BF as charged trapping layer, the N-BF system could be generated the positive charges at the surface of Nylon but not recombined with electron at electrode because it can be deeply trapped in the band of BF charge-trapping layer. Thus, having a charge-trapping layer contains more time to store the charges before combining with the electrons at the CNT electrode, as shown in Figure 6(e) (ii). It corresponds to higher surface potential and the holding of voltage of N-BF multilayer T-TENG. The more understanding about deep trapping process in TENG is discussed and explained deeply elsewhere (Jiang *et al*., 2020).

To evaluate its practical applicability, a conventional full-wave rectifier (FWR) circuit

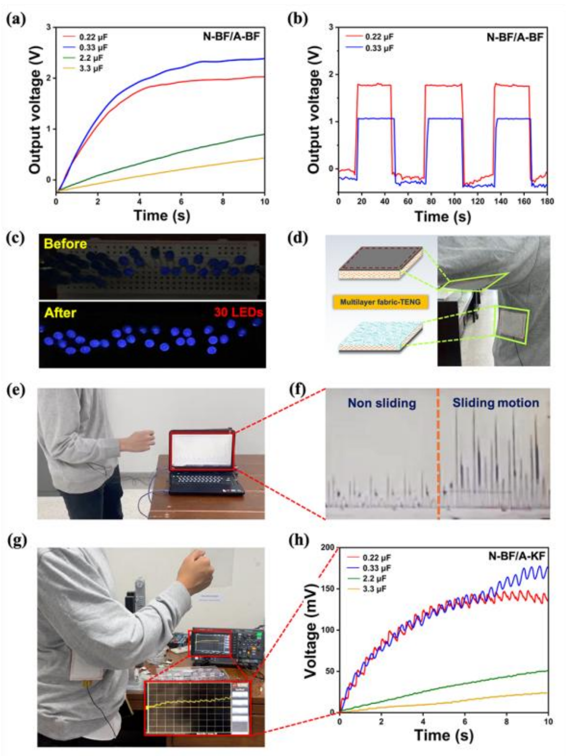

Figure 7. **(a) Capacitor chargeability, (b) Charge-discharged cycles, and (c) 30 driven LEDs of nylon/acrylic fabric based TENG with BF as multilayer structure. (d) The application of nylon/acrylic fabric with fiber-inserted intermediate layers in the fabrication process with (e) the device's sensor testing and (f) sensor values. (g) Chargeability testing and (h) chargeability results of nylon/acrylic fabric with fiber-inserted intermediate layers**

we employed to connect between the T-TENG and capacitor. The multilayer T-TENG within N-BF/A-KF system was used to charge the different capacity of capacitor, which included 0.22, 0.33, 2.2, and 3.3 µF. The resulting charge curves, displayed in Figure 7(a), illustrate that during the charging period, 0.22 µF and 0.33 µF capacitors could reach around 2 V and 2.4 V within approximately 7 and 9 seconds. Nevertheless, the 2.2 µF and 3.3 µF capacitors could not be fully charged within the same 10 s, and only reached 0.9 V and 0.4 V within this period. The charge-discharge cycles are presented in Figure 7(b), illustrating the stability of charge-discharged ability. To test the operation of T-TENG for small power supply, the LED was connected to the N-BF/A-KF T-TENG directly to assess real-time power supply capabilities, as displayed schematically in Figure 7(c). The results indicate that the multilayer T-TENG can power approximately 30 blue LEDs. Moreover, according to Figure 7(d), the multilayer T-TENG module within 5 × 5 cm^2 was integrated to the long-sleeved garments, trying to operate by mechanical force from human motion. The experiments and data analysis regarding the electrical output performance after sliding by running have shown promising results. Sliding the T-TENG by human movement (Figure 7(e)), *i.e.*, walk and run can generate signal waveforms distinguishably when comparing to stand still. The signal appears clearly when body movement or acceleration occurs as shown in Figure 7(f). In addition, Figure 7(g) and h exhibited the chargeability of long-sleeved garments T-TENG by running. The results demonstrate the charging period of 0.22, 0.33, 2.2, and 3.3 µF capacitors. It could fully-charge at 0.22 µF and 0.33 µF and reach around 140 mV and 170 mV, respectively, within 7 s. These findings indicate a promising direction for the production and development of self-powered sensors and energy harvesters for real-time monitoring devices capable of real-world applications in the future.

Conclusions

This research has achieved significant success in designing woven fabrics of nylon and acrylic system utilizing for T-TENG by further engineering multilayer structures to enhance its electrical output performance. The investigation of different weaving patterns reveals the different surface contact areas, which is a crucial factor that impacts on the T-TENG's electrical output performance. After testing with three material systems, including nylon-Teflon, Al-acrylic and nylon-acrylic, weaving fabric within matt weave pattern shows highest surface contact area. Higher surface area makes fabric deform more easily, increasing the more point of contacting to induce triboelectrification, generating more triboelectric charges. For fully-fabric T-TENG, pairing between nylon-acrylic could achieved the output efficiency of ~5.5 V and ~510 nA. The further significant enhancement on T-TENG's performance is in accordance with the deep traps process by inserting intermediate charge-trapping layer of polyester fiber and kapok (lignocellulosic) fiber. The results indicate that multilayer structure could generate higher output efficiency. The temporary charges diffusion from the surface to re-combine at electrodes is blocked by adding intermediate layer, facilitating the fast saturation of electrostatic induction to increase difference potential. By taking this advantage high stretchability and flexibility of fully-fabric systems could be fabricated to be a high triboelectric performance. By rubbing the nylon/ball fiber with acrylic/kapok, the output of V_{OC} and I_{SC} at ~16.2 V, ~4.8 µA is reached, which is 3 and 8 times higher than the fabric T-TENG without intermediate layer of fiber. For the application section of attaching the device at the long-sleeved garments, the fully-chargeability with 0.22 µF and 0.33 µF capacitors, 30 LEDs driving, and signals testing with basic sensor were demonstrated. This work demonstrates the paved way for enhancing fully-fabric T-TENG using simple method design and engineering, promising the direction to produce T-TENG for real-world applications in the next-generation human-oriented wearable electronics.

Acknowledgments

The work of Thitirat Charoonsuk was supported by the National Research Council of Thailand (NRCT) through Grant Number N42A650220 and Srinakharinwitor University, Faculty of Science under the 214/2566 grant. Suwan Plaipichit's contribution to the study was funding by Faculty of Science, Srinakharinwirot University under the Grant Number 215/2566. The work of N. Vittayakorn was financial support from KMITL under Grant No. KREF116501 and 2567-02-05-020. The authors also would like to thank Ms. Natchaya Kerdsoonthorn, Ms. Arisa Nikomkhet and Mr. Chanachot Saetang for their assisting with sample preparation and electrical output measurement.

References

Bairagi, S., Khandelwal, G., Karagiorgis, X., Gokhool, S., Kumar, C., Min, G., and Mulvihill, D.M. (2022). High-performance triboelectric nanogenerators based on commercial textiles: Electrospun nylon 66 nanofibers on silk and PVDF on polyester. ACS Applied Materials & Interfaces, 14(39):44591-44603. https://doi.org/10.1021/acsami.2c13092

Bhattacharya, S., and Chaudhari, D.S. (2014). Study on structural, mechanical and functional properties of polyester silica nanocomposite fabric. International Journal of Pure and Applied Sciences and Technology, 21:43-52.

Charoonsuk, T., Muanghlua, R., Sriphan, S., Pongampai, S., and Vittayakorn, N. (2021b). Utilization of commodity thermoplastic polyethylene (PE) by enhanced sensing performance with liquid phase electrolyte for a flexible and transparent triboelectric tactile sensor. Sustainable Materials and Technologies, 27:e00239. https://doi.org/10.1016/j.susmat.2020.e00239

Charoonsuk, T., Pongampai, S., Pakawanit, P., and Vittayakorn, N. (2021a). Achieving a highly efficient chitosan-based triboelectric nanogenerator via adding organic proteins: Influence of morphology and molecular structure. Nano Energy, 89(Part B):106430. https://doi.org/10.1016/j.nanoen.2021.106430

Chen, J., Guo, H., Pu, X., Wang, X., Xi, Y., and Hu, C. (2018). Traditional weaving craft for one-piece self-charging power textile for wearable electronics. Nano Energy, 50:536-543. https://doi.org/10.1016/j.nanoen.2018.06.009

Cui, N., Gu, L., Lei, Y., Liu, J., Qin, Y., Ma, X., Hao, Y., and Wang, Z.L. (2016). Dynamic behavior of the triboelectric charges and structural optimization of the friction layer for a triboelectric nanogenerator. ACS Nano, 10(6):6131-6138. https://doi.org/10.1021/acsnano.6b02076

Feng, Y., Zheng, Y., Zhang, G., Wang, D., Zhou, F., and Liu, W. (2017). A new protocol toward high output TENG with polyimide as charge storage layer. Nano Energy, 38:467-476. https://doi.org/10.1016/j.nanoen.2017.06.017

Jeong, J., Kwon, J.-H., Lim, K., Biswas, S., Tibaldi, A., Lee, S., Oh, H. J., Kim, J.-H., Ko, J., Lee, D.-W., Cho, H., Lang, P., Jang, J., Lee, S., Bae, J.-H., and Kim, H. (2019). Comparative study of triboelectric nanogenerators with differently woven cotton textiles for wearable electronics. Polymers, 11(9):1443. https://doi.org/10.3390/polym11091443

Jiang, H., Lei, H., Wen, Z., Shi, J., Bao, D., Chen, C., Jiang, J., Guan, Q., Sun, X., and Lee, S.-T. (2020). Charge-trapping-blocking layer for enhanced triboelectric nanogenerators. Nano Energy, 75:105011. https://doi.org/10.1016/j.nanoen.2020.105011

Kartina, A.K.S., and Suhaila, M.H.N. (2012). Oil sorption capacity of kapok fiber. In 2012 IEEE Colloquium on Humanities, Science and Engineering (CHUSER) (pp. 876-878). IEEE. https://doi.org/10.1109/CHUSER.2012.6504439

Kavita, M., and Abdel-Fattah, S. (2011). Color and weave relationship in woven fabrics. In S. Vassiliadis (Ed.), Advances in modern woven fabrics technology (Chapter 7). IntechOpen.

Khwanming, R., Pongampai, S., Vittayakorn, N., and Charoonsuk, T. (2023). Cellulose-based fabrics triboelectric nanogenerator: Effect of fabric microstructure on its electrical output. Journal of Metals, Materials and Minerals, 33(3):1673. https://doi.org/10.55713/jmmm.v33i3.1673

Kim, D.W., Lee, J.H., You, I., Kim, J.K., and Jeong, U. (2018). Adding a stretchable deep-trap interlayer for high-performance stretchable triboelectric nanogenerators. Nano Energy, 50:192-200. https://doi.org/10.1016/j.nanoen.2018.05.041

Kim, Y.J., Lee, J., Park, S., Park, C., Park, C., and Choi, H.-J. (2017). Effect of the relative permittivity of oxides on the performance of triboelectric nanogenerators. RSC Advances, 7(78):49368-49373. https://doi.org/10.1039/C7RA07274K

Kingsbury, C.A. (2019). The inductive effect in organic chemistry. University of Nebraska-Lincoln.

Koto, N., and Soegijono, B. (2019). Effect of rice husk ash filler of resistance against of high-speed projectile impact on polyester-fiberglass double panel composites. Journal of Physics: Conference Series, 1191(1):012058. https://doi.org/10.1088/1742-6596/1191/1/012058

Lin, S., Xu, C., Xu, L., and Wang, Z.L. (2020). The overlapped electron-cloud model for electron transfer in contact electrification. Advanced Functional Materials, 30(11):1909724. https://doi.org/10.1002/adfm.201909724

Liu, Y., Mo, J., Fu, Q., Lu, Y., Zhang, N., Wang, S., and Nie, S. (2020). Enhancement of triboelectric charge density by chemical functionalization. Advanced Functional Materials, 30(50):2004714. https://doi.org/10.1002/adfm.202004714

Menge, H.G., Kim, J.O., and Park, Y.T. (2020). Enhanced triboelectric performance of modified PDMS nanocomposite multilayered nanogenerators. Materials, 13(18):4156. https://doi.org/10.3390/ma13184156

Niu, S., and Wang, Z.L. (2015). Theoretical systems of triboelectric nanogenerators. Nano Energy, 14:161-192. https://doi.org/10.1016/j.nanoen.2014.11.034

Niu, S., Liu, Y., Wang, S., Lin, L., Zhou, Y.S., Hu, Y., and Wang, Z.L. (2013). Theory of sliding-mode triboelectric nanogenerators. Advanced Materials, 25(43):6184-6193. https://doi.org/10.1002/adma.201302808

Paosangthong, W., Wagih, M., Torah, R., and Beeby, S. (2019). Textile-based triboelectric nanogenerator with alternating positive and negative freestanding grating structure. Nano Energy, 66:104148. https://doi.org/10.1016/j.nanoen.2019.104148

Peng, X., Dong, K., Ning, C., Cheng, R., Yi, J., Zhang, Y., Sheng, F., Wu, Z., and Wang, Z.L. (2021). All-nanofiber self-powered skin-interfaced real-time respiratory monitoring system for obstructive sleep apnea-hypopnea syndrome diagnosing. Advanced Functional Materials, 31(34):2103559. https://doi.org/10.1002/adfm.202103559

Saleem, M., Naz, M.Y., Shoukat, B., Shukrullah, S., and Hussain, Z. (2021). Functionality and applications of non-thermal plasma activated textiles: A review. Materials Today: Proceedings, 47:S74-S82. https://doi.org/10.1016/j.matpr.2020.05.158

Somkuwar, V.U., Pragya, A., and Kumar, B. (2020). Structurally engineered textile-based triboelectric nanogenerator for energy harvesting application. Journal of Materials Science, 55(12):5177-5189. https://doi.org/10.1007/s10853-020-04359-2

Sun, T., Zhou, B., Zheng, Q., Wang, L., Jiang, W., and Snyder, G. J. (2020). Stretchable fabric generates electric power from woven thermoelectric fibers. Nature Communications, 11(1):572. https://doi.org/10.1038/s41467-020-14399-6

Ukasi, S., Jutapukti, P., Ninthub, C., Pinpru, N., Pakawanit, P., Vittayakorn, W., Pongampai, S., Vittayakorn, N., and Charoonsuk, T. (2024). Gamma glycine enhances efficiency of organic hybrid piezoelectric-triboelectric nanogenerators. Nano Energy, 119:109045. https://doi.org/10.1016/j.nanoen.2023.109045

Xie, X., Chen, X., Zhao, C., Liu, Y., Sun, X., Zhao, C., and Wen, Z. (2021). Intermediate layer for enhanced triboelectric nanogenerator. Nano Energy, 79:105439. https://doi.org/10.1016/j.nanoen.2020.105439

Yang, Y., Xie, L., Wen, Z., Chen, C., Chen, X., Wei, A., Cheng, P., Xie, X., and Sun, X. (2018). Coaxial triboelectric nanogenerator and supercapacitor fiber-based self-charging power fabric. ACS Applied Materials & Interfaces, 10(49):42356-42362. https://doi.org/10.1021/acsami.8b15104

Younes, B. (2023). Smart E-textiles: A review of their aspects and applications. Journal of Industrial Textiles, 53:15280837231215493. https://doi.org/10.1177/15280837231215493

Zhao, Z., Yan, C., Liu, Z., Fu, X., Peng, L.-M., Hu, Y., and Zheng, Z. (2016). Machine-washable textile triboelectric nanogenerators for effective human respiratory monitoring through loom weaving of metallic yarns. Advanced Materials, 28(46):10267-10274. https://doi.org/10.1002/adma.201603679

Zhou, T., Zhang, C., Han, C.B., Fan, F.R., Tang, W., and Wang, Z.L. (2014). Woven structured triboelectric nanogenerator for wearable devices. ACS Applied Materials & Interfaces, 6(16):14695-14701. https://doi.org/10.1021/am504110u

Zhu, G., Peng, B., Chen, J., Jing, Q., and Lin Wang, Z. (2015). Triboelectric nanogenerators as a new energy technology: From fundamentals, devices, to applications. Nano Energy, 14:126-138. https://doi.org/10.1016/j.nanoen.2014.11.050

Zhu, M., Shi, Q., He, T., Yi, Z., Ma, Y., Yang, B., Chen, T., and Lee, C. (2019). Self-powered and self-functional cotton sock using piezoelectric and triboelectric hybrid mechanism for healthcare and sports monitoring. ACS Nano, 13(2):1940-1952. https://doi.org/10.1021/acsnano.8b08329